

# Pseudoresonance mechanism of all-optical frequency standard operation

G.Kazakov<sup>1</sup>, B.Matisov<sup>1</sup>, I.Mazets<sup>2</sup>, G.Mileti<sup>3</sup>, J.Delporte<sup>4</sup>

<sup>1</sup>*St. Petersburg State Polytechnic University, St. Petersburg, 195251, Russia*

<sup>2</sup>*A.F. Ioffe Physics-Technical Institute, St. Petersburg 194021, Russia*

<sup>3</sup>*Observatoire Cantonal Neuchâtel, 2000 Neuchâtel, Switzerland*

<sup>4</sup>*Centre National d'Etudes Spatiales, 31401 Toulouse, France*

We propose a novel approach to all-optical frequency standard design, based on a counterintuitive combination of the coherent population trapping effect and signal discrimination at the maximum of absorption for the probe radiation. The short-term stability of such a standard can achieve the level of  $10^{-14}/\sqrt{\tau}$ . The physics beyond this approach is dark resonance splitting caused by interaction of the nuclear magnetic moment with the external magnetic field.

PACS numbers: 06.30.Ft, 42.50.Gy, 32.80.Bx

The unit of time in the Système International (the second) is defined via the period of the transition between the hyperfine (HF) components of the ground state of the  $^{133}\text{Cs}$  atom (in the limit of vanishing external perturbations). Secondary standards may use other elements (alkali metals, hydrogen). Operation of a frequency standard is provided by locking a microwave signal produced by a quartz crystal oscillator to a resonance on the transition between the working levels [1], i. e. the Zeeman components of the HF structure with zero projection of the total angular momentum. Such a choice of the working levels is dictated by the absence of the linear Zeeman shift. The resonance can be excited by direct microwave transition or by two-photon Raman transition. The latter option provides the basis for all-optical frequency standards [2, 3, 4, 5, 6, 7, 8] where the setup includes no microwave cavities, but electro-optical modulation of the laser beam or direct modulation of the diode laser current are used instead.

If the interaction time of an atom with the laser field exceeds few optical pumping cycles then the coherent population trapping (CPT) sets in, giving rise to the so-called dark resonance [9, 10]. The physical reason for the CPT is optical pumping of atoms into a coherent superposition of the two ground state sublevels, which is immune to excitation by the frequency-split laser radiation. The CPT leads to decrease of absorption of the laser light. However, if the Raman detuning (the difference between the frequency splitting of the two-component laser radiation and the transition frequency between the two ground state sublevels) exceeds the dark resonance width (what can be as small as few dozens Hz [6, 11]), the CPT atomic state is destroyed, and usual value of the laser radiation absorption is restored.

Keeping the frequency of a generator that provides laser frequency splitting coincident with the position of the dark resonance on the working transition is the physical mechanism of the frequency standardization by optical means.

In the present paper we propose a different, quite counterintuitive technique. No specific resonance on the working transition is excited. Instead, its frequency is identified as *the position of maximum absorption between the*

*two side dark resonances involving magnetically-sensitive Raman transitions.*

Before to proceed further, we have to recall some basic ideas from the theory of CPT in systems with a closed-loop interaction contour [12]. An example of such a system is given in Fig. 1.

The reason why  $\sigma^+/\sigma^-$ -configuration of the laser radiation polarizations is used, instead of simply applying  $\sigma^+$ -polarized light only, is the adverse influence of the states with the maximum projection of the angular momentum, where most of the atoms are accumulated, this drastically reducing the dark resonance contrast and, hence, worsening the standard's performance.

Consider the pair of the ground (g) state sublevels,  $|F_g = F, m_g = m\rangle$  and  $|F_g = F + 1, m_g = m\rangle$ , each of them resonantly coupled to the first excited (e) state sublevels  $|F_e = F, m_e = m + 1\rangle$  and  $|F_e = F, m_e = m - 1\rangle$  (or  $|F_e = F + 1, m_e = m + 1\rangle$  and  $|F_e = F + 1, m_e = m - 1\rangle$ ), this forming so-called double  $\Lambda$  closed loop interaction contour. Here  $F$  is the total angular momentum of the given HF component,  $m$  is the angular momentum projection to the quantization axis. The interaction matrix element for the transition  $|F_g, m_g\rangle \leftrightarrow |F_e, m_e\rangle$  is

$$\langle F_g, m_g | \hat{V} | F_e, m_e \rangle = -\langle F_g, m_g | \hat{d}_q | F_e, m_e \rangle E_{F_g, F_e, q}, \quad (1)$$

where  $E_{F_g, F_e, q}$  is the complex amplitude of the laser field resonant to the given transition,  $q = m_e - m_g$  denotes the cyclic component of the polarization unit vector, and the electric dipole element can be represented, according to the Wigner-Eckart theorem [13] as

$$\langle F_g, m_g | \hat{d}_q | F_e, m_e \rangle = (-1)^{F_g + J_e + I - 1} \sqrt{2F_g + 1} \times C_{F_g m_g 1 q}^{F_e m_e} \left\{ \begin{matrix} J_g & I & F_g \\ F_e & 1 & J_e \end{matrix} \right\} \langle J_g || \hat{d} || J_e \rangle, \quad (2)$$

where  $J_{g(e)}$  is the electronic angular momentum of the ground (excited) state,  $I$  is the nuclear spin,  $C_{F_g m_g 1 q}^{F_e m_e}$  is the Clebsch-Gordan coefficient,  $\left\{ \begin{matrix} J_g & I & F_g \\ F_e & 1 & J_e \end{matrix} \right\}$  is the  $6j$ -symbol, and  $\langle J_g || \hat{d} || J_e \rangle$  is the reduced matrix element of the dipole moment.

Consider the two  $\Lambda$ -schemes produced by the laser radiation with  $\sigma^+$  and  $\sigma^-$  polarizations separately. The

two corresponding CPT states,  $|CPT_+\rangle$  and  $|CPT_-\rangle$ , can be identified as

$$\begin{aligned} |CPT_\pm\rangle = & \left( \langle F_g = F + 1, m | \hat{V} | F_e, m \pm 1 \rangle | F_g = F, m \rangle - \right. \\ & \left. - \langle F_g = F, m | \hat{V} | F_e, m \pm 1 \rangle | F_g = F + 1, m \rangle \right) \times \\ & \times \left( |\langle F_g = F, m | \hat{V} | F_e, m \pm 1 \rangle|^2 + \right. \\ & \left. + |\langle F_g = F + 1, m | \hat{V} | F_e, m \pm 1 \rangle|^2 \right)^{-1/2}. \end{aligned} \quad (3)$$

Let  $\varsigma$  be a parameter defined via the relation

$$\begin{aligned} \frac{\langle F_g = F + 1, m | \hat{V} | F_e, m + 1 \rangle}{\langle F_g = F, m | \hat{V} | F_e, m + 1 \rangle} = \\ = \varsigma \frac{\langle F_g = F + 1, m | \hat{V} | F_e, m - 1 \rangle}{\langle F_g = F, m | \hat{V} | F_e, m - 1 \rangle}. \end{aligned} \quad (4)$$

If the amplitude and phase conditions [12, 14] for the complex interaction matrix elements are satisfied, i. e.  $\varsigma = +1$ , then the two states defined by Eq. (3) coincide, and we get perfect CPT in the double  $\Lambda$ -scheme. Then, if we scan the Raman detuning across the resonance, the dark resonance in the absorption spectrum appears [15]. In the contrary, if  $\varsigma = -1$  then  $|CPT_+\rangle$  is the state corresponding to maximally enhanced absorption of the  $\sigma^-$ -polarized radiation, and *vice versa*. It makes CPT in such a double  $\Lambda$ -scheme impossible. A simple but a bit lengthy analysis shows that no structure appears in the absorption spectrum near the resonance, *if no other ground state sublevels are taken into account*.

Unfortunately, satisfying the condition  $\varsigma = +1$  implies sophisticated experimental techniques. Indeed, if all the four components of the laser radiation, different in polarization and frequency, are obtained from the same input light beam by electro-optical modulator without specific precautions, one gets  $E_{F, F_e, +1}/E_{F+1, F_e, +1} = E_{F, F_e, -1}/E_{F+1, F_e, -1}$ . Due to the general property of Clebsch-Gordan coefficients [13], we always get for the working transition

$$\begin{aligned} \langle F, 0 | \hat{d} | F_e, +1 \rangle / \langle F + 1, 0 | \hat{d} | F_e, +1 \rangle = \\ = - \langle F, 0 | \hat{d} | F_e, -1 \rangle / \langle F + 1, 0 | \hat{d} | F_e, -1 \rangle \end{aligned} \quad (5)$$

that results in  $\varsigma = -1$ . Therefore one has to introduce a  $\pi$  phase shift to the  $\sigma^-$ -component of the laser radiation, with respect to  $\sigma^+$  one. One solution, implemented by the NIST group [7, 16], is based on counterpropagating configuration of  $\sigma^+$ - and  $\sigma^-$ -polarized beams. In this case, the CPT condition  $\varsigma = +1$  is satisfied in periodically located spatial regions, which are quite narrow (much less than a quarter of the HF transition wavelength). It limits the cell size by  $\sim 1$  mm. Dark resonance in such a miniaturized cell are quite broad, and the corresponding short-term stability of a frequency standard is limited by

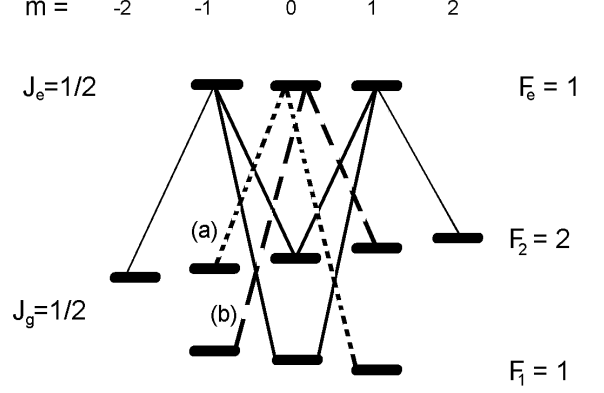


FIG. 1: Scheme of optically-induced transitions in  $^{87}\text{Rb}$  atom, case of  $F_e = 1$ . “Closed loops” involving the working (0-0) transition are shown by bold solid black lines. Additional  $\Lambda$ -schemes are shown by (a) dotted lines (the pair of ground state Zeeman sublevels  $|F_g = 1, m = +1\rangle$ ,  $|F_g = 2, m = -1\rangle$  being involved), and (b) dashed lines ( $|F_g = 1, m = -1\rangle$ ,  $|F_g = 2, m = +1\rangle$  being involved).

$\sim 10^{-11}/\sqrt{\tau}$  [3, 7],  $\tau$  being the integration time (in seconds). Recently high-contrast dark resonance have been demonstrated using so-called “push-pull” technique [17], where a set of  $\lambda/4$  plates, polarization-sensitive beam splitters and reflectors provides the necessary phase shift in the cw regime. The “lin  $\perp$  lin” technique developed by Zanon et. al. [18] realizes a similar idea in time-domain (Ramsey) spectroscopy. The setups of Refs. [17, 18] are quite good for high-precision *laboratory* frequency standards. However, it is quite desirable to design a simpler in construction and easier to handle all-optical frequency standard, more suitable, e.g., for operation on board of a satellite or in other mobile instrument applications. In the present paper we propose a relevant approach.

We have obtained an intriguing result: the “adverse” condition  $\varsigma = -1$  itself, holding for  $m = 0$ , does not prevent precise spectroscopic identification of the working transition frequency and locking to it a quartz generator. The key factor here is the influence of the other Zeeman sublevels of the HF structure of the ground state. For the sake of definiteness, let us consider gas of  $^{87}\text{Rb}$  atoms placed in a homogeneous magnetic field  $\mathbf{H}$ . A linearly polarized laser radiation propagates along  $\mathbf{H}$ . Its carrier frequency and modulation frequency are chosen so that the  $F_g = 1 \leftrightarrow F_e = 1$  and  $F_g = 2 \leftrightarrow F_e = 1$  components of the  $D_1$ -line are excited. Being projected to the quantization axis defined by the magnetic field, the linear polarization is represented by the coherent superposition of  $\sigma^+$  and  $\sigma^-$ -polarizations, see Fig. 1. Since there is no delay line for the  $\sigma^+$ -polarized component, we have  $\varsigma = -1$  for  $m = 0$ , and the corresponding double  $\Lambda$ -scheme (shown by bold lines in Fig. 1) exhibit no CPT resonance. However, there are two additional  $\Lambda$ -schemes, corresponding

to quadrupole ( $|\Delta m| = 2$ ) two-photon transitions and involving the pairs of Zeeman sublevels  $\{|F_g = 1, m = +1\rangle, |F_g = 2, m = -1\rangle\}$ , indicated by (a) Fig. 1, and  $\{|F_g = 1, m = -1\rangle, |F_g = 2, m = +1\rangle\}$ , indicated by (b) in Fig. 1. The distances between these ground state Zeeman sublevels in the weak magnetic field  $H$  are [1]

$$\omega_{a,b} = \omega_{hfs} \pm \frac{2g_I\mu_N}{\hbar}H + \frac{3g_J^2\mu_B^2}{8\omega_{hfs}\hbar^2}H^2, \quad (6)$$

where  $\omega_{hfs}$  is the hyperfine splitting frequency of the ground state HF components in the absence of magnetic field,  $\mu_B = e\hbar/(2m_e c)$  is the Bohr magneton,  $\mu_N = e\hbar/(2m_p c)$  is the nuclear magneton,  $g_I = \mu/\mu_N$  is the nuclear Landé factor,  $g_J$  is the electronic Landé factor,  $\mu$  is the magnetic momentum of atomic nucleus. The positive sign of the second term in the right-hand-side of Eq. (6) corresponds to the  $\Lambda$ -scheme denoted in Fig. 1 by (a), the negative sign corresponds to the scheme (b). Note that one may erroneously treat these side dark resonances as magnetically insensitive in the linear approximation, if one does not take into account the magnetic moment of the nucleus, since the linear Zeeman shifts due to the electronic magnetic moment for each state in the pair  $|F_g = 1, m = \pm 1\rangle, |F_g = 2, m = \mp 1\rangle$  are the same. Observation of splitting of dark resonances due to interaction of nuclear spins with external magnetic field was first reported in Ref. [19] for Cs atoms, and recently [20] for  $^{87}\text{Rb}$  atoms. In Eq. (6) we retain, for the sake of generality, the second-order Zeeman effect terms.

Therefore, magnetic field shifts the positions of the corresponding dark resonances close to the working transition. The two dark resonances are symmetric (to the second order Zeeman effect) with respect to the position of the  $|F_g = 1, m = 0\rangle \leftrightarrow |F_g = 2, m = 0\rangle$  working transition. If the magnetic field shift is small (in comparison with single resonance width), the two dark resonances are not resolved, see Fig. 2, the dotted curve. For intermediate values of  $H$  they are resolved partially, thus forming a minimum in the transmission spectrum exactly between them, see Fig. 2, the solid curve. The position of this minimum coincides with the frequency of the  $|F_g = 1, m = 0\rangle \leftrightarrow |F_g = 2, m = 0\rangle$  transition and can be implemented in discriminator of an all-optical frequency standard. Such a structure formed between two maxima in the transmission spectrum can be called a *pseudoresonance*. The minimum width of the pseudoresonance is of the order of the dark resonance width. Further increase of  $H$  makes the two dark resonances fully resolved. As a result, the bottom of the pseudoresonance dip becomes flat, which is unsuitable for the frequency standardization purposes, see Fig. 2, the dot-dashed curve. The second-order Zeeman shift of the pseudoresonance is of order of the same shift for the working transition.

The light shift of the pseudoresonance position is the same as that of each of the two side dark resonances [22, 23]. In particular, it vanishes if the laser is tuned exactly in resonance with the  $F_e = 1$  component of the  $^{87}\text{Rb}$  D<sub>1</sub>-line.

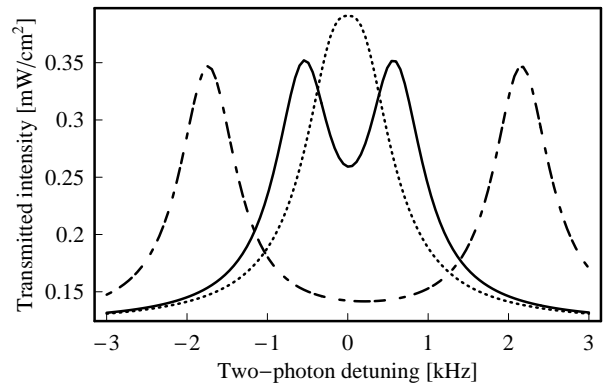


FIG. 2: Transmission spectrum of the cell with the parameters specified in the text. Incident radiation intensity  $U_0 = 0.5 \text{ mW/cm}^2$ . The excitation scheme is shown in Fig. 1. Dotted line corresponds to  $H = 0.05 \text{ G}$ , solid line corresponds to  $H = 0.2 \text{ G}$ , dot-dashed line corresponds to  $H = 0.7 \text{ G}$ .

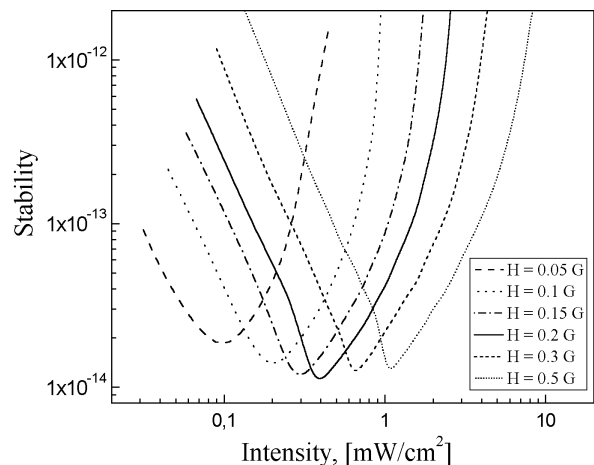


FIG. 3: Frequency standard stability (Allan deviation, dimensionless) for the integration time  $\tau = 1 \text{ s}$  versus laser field intensity for different magnetic fields.

Note that the  $F_e = 2$  component of the  $^{87}\text{Rb}$  D<sub>1</sub> line can not be used for pseudoresonance creation, since in this case the states  $|F_e = 2, m = \pm 2\rangle$  are excited thus turning the relevant  $\Lambda$ -schemes into  $W$ -type schemes, in which CPT is not possible [9]. D<sub>2</sub>-line is also unsuitable because of the small magnitude of the HF splitting of the  $5^2P_{3/2}^o$  excited state and, hence, strong overlapping of Doppler contours of optical transitions to different HF components of the excited state.

We performed numerical simulations of linearly-polarized, two-component laser light propagation through a  $^{87}\text{Rb}$  gas cell with the following parameters: radius  $R_c = 1 \text{ cm}$ , length  $L_c = 2.5 \text{ cm}$ , number density  $n = 1.1 \times 10^{11} \text{ cm}^{-3}$  ( $T = 327 \text{ K}$ ), the diffusion coefficient for  $^{87}\text{Rb}$  atoms  $D = 20 \text{ cm}^2/\text{s}$  corresponding to the buffer gas ( $\text{N}_2$ ) pressure = 15 Torr (such a pressure

is chosen to provide quenching of the excited state and thus diminish rescattering of photons). The relaxation rate  $\Gamma$  of ground state coherences in such a cell is dominated by wall collisions [1] and can be estimated as  $\Gamma \approx 300 \text{ s}^{-1}$ . In the present paper we do not discuss the effect of pressure shift of the HF transition [1, 21] and the choice of an optimum buffer gas mixture, postponing this subject to a more extended publication. However, we aware that one has to minimize the thermal dependence of the pressure shift, especially for improving the long-term stability of the standard. As concerns Fig. 2, the pressure shift at the specified cell temperature is included there into the working transition frequency value for zero magnetic field. The density matrix formalism for the whole manifold of the states was applied. The results are shown in Fig. 2. Apparently, the width of the absorption peak of about 0.7 kHz is achievable simultaneously with the contrast  $\sim 30 \%$ . In Fig. 3 we plot the stability  $\sigma_y$  of the standard based on the *pseudoresonance* discrimination method versus the incident radiation intensity for different values of external magnetic fields [1]:

$$\sigma_y \approx \left( \omega_{hfs} |S''(0)| W f(\Theta) \sqrt{\frac{P\tau}{\hbar\omega_0}} \right)^{-1}, \quad (7)$$

where  $P = U_0 A$  is the total laser radiation power,  $U_0$  being the intensity at the cell input, and  $A$  being the effective beam cross-section area (in our simulations we assume that the laser beam is wide enough to provide  $A \approx \pi R_c^2$ ),  $\tau$  is the integration time,  $\omega_0$  is the  $D_1$ -line

resonance frequency,  $S''(0)$  is the second derivative of the signal over the two-photon (Raman) detuning at the extremum of the reference spectroscopic line (in our case, at the pseudoresonance position),  $W$  is the width of the detuning range where  $S''$  is approximately constant. The signal  $S$  is the transmitted laser power normalized to its value outside the CPT-resonance induced structure but still within the Doppler profile of the  $D_1$ -line. The function  $f(\Theta)$  is close to 1 in the optimal range of values of the cell optical thickness  $\Theta$  ( $0.5 < \Theta < 1$ ). Standard stability estimation shows that short-term stability  $\sigma_y \sim 10^{-14}/\sqrt{\tau}$  is achievable.

To conclude, we demonstrate theoretically the existence of a novel structure in a laser-light transmission spectrum under the CPT condition, a *pseudoresonance*, that is a narrow (having the width much less than the natural width of the excited state) absorption maximum between the two dark resonances involving  $m = \pm 1$  sub-levels of the ground state of an alkali atom, while CPT in the double  $\Lambda$ -scheme based on  $m = 0$  is absent. The performance of an all-optical frequency standard using this effect for signal discrimination must be the same, as that of a standard employing the “push-pull” technique [17]. However, a pseudoresonance-based standard is to be easier in both construction and handling and thus more suitable for application on board of a satellite or in other mobile instrument applications.

This research is supported by the INTAS-CNES, project 03-53-5175, and by the Ministry of Education and Science of Russia, project UR.01.01.287. We thank V. Yudin and D. Sarkisyan for helpful discussion.

- 
- [1] J. Vanier and C. Audoin, *The Quantum Physics of Atomic Frequency Standards*, (A. Hilger, Bristol, 1989).
  - [2] N. Cyr, M. Tetu, and M. Breton, *IEEE Trans. Instrum. Meas.* **42**, 640 (1993).
  - [3] J. Kitching et al., *IEEE Trans. Instrum. Meas.* **49**, 1313 (2000).
  - [4] J. Kitching, S. Knappe, and L. Hollberg, *Appl. Phys. Lett.* **81**, 553 (2002).
  - [5] M. Stahler et al., *Optics Letters* **27**, 1472 (2002).
  - [6] M. Merimaa, T. Lindvall, I. Tittonen, and E. Ikonen, *JOSA B* **20**, 273 (2003).
  - [7] S.V. Kargapol'tsev et al., *Laser Phys. Lett.* **1**, 495 (2004).
  - [8] S. Knappe et al., *Optics Express* **13**, 1249, (2005).
  - [9] B.D. Agap'ev, M. B. Gorny, B. G. Matisov, and Yu. V. Rozhdestvensky, *Physics – Uspekhi* **36**, 763, (1993).
  - [10] E. Arimondo, in: *Progress in Optics*, ed. E. Wolf, **35** (North Holland, Amsterdam, 1996), p.257.
  - [11] S. Brandt, A. Nagel, R. Wynands, and D. Meschede, *Phys. Rev. A* **56**, R1063 (1997).
  - [12] D. V. Kosachev, B. G. Matisov, and Yu. V. Rozhdestvensky, *J. Phys. B* **25**, 2473 (1992).
  - [13] D. A. Varchalovich, A. N. Moskalev, and V. K. Kheronsky, *Quantum Theory of Angular Momentum* (World Scientific, Singapore, 1988).
  - [14] V. Taichenachev, V. I. Yudin, V. L. Velichansky, and S. A. Zibrov, arXiv: quant-ph/0503036.
  - [15] W. Maichen et. al., *Phys. Rev. A* **53**, 3444 (1996).
  - [16] A.V. Taichenachev et. al., *JETP Letters* **80**, 236, (2004).
  - [17] Y.-Y. Jau et. al, *Phys. Rev. Lett.* **93**, 160802, (2004).
  - [18] T. Zanon et.al., *Phys.Rev.Lett.* **94**, 193002, (2005).
  - [19] S. Knappe et al., *Phys. Rev. A* **61**, 012508 (1999).
  - [20] S.A. Zibrov et al., *Abstract Book of ICONO'05* (St.Petersburg, May 2005), p.ISK8; V.A. Taichenachev, V.I. Yudin, V.L. Velichansky, and S.A. Zibrov, arXiv: quant-ph/0507090.
  - [21] L.B. Robinson, *Phys. Rev.* **117**, 1275 (1960).
  - [22] A. Nagel, S. Brandt, D. Meschede, and R. Wynands, *Europhys. Lett.* **48**, 385 (1999).
  - [23] F. Levi, A. Godone, and J. Vanier, *IEEE Trans. Ultrason. Ferroelectr. Frequency Control* **47**, 466 (2000).